

## Relevance of the Thorpe length scale in stably stratified turbulence

Benjamin D. Mater, Simon M. Schaad, and Subhas Karan Venayagamoorthy

Citation: *Phys. Fluids* **25**, 076604 (2013); doi: 10.1063/1.4813809

View online: <http://dx.doi.org/10.1063/1.4813809>

View Table of Contents: <http://pof.aip.org/resource/1/PHFLE6/v25/i7>

Published by the AIP Publishing LLC.

---

### Additional information on Phys. Fluids

Journal Homepage: <http://pof.aip.org/>

Journal Information: [http://pof.aip.org/about/about\\_the\\_journal](http://pof.aip.org/about/about_the_journal)

Top downloads: [http://pof.aip.org/features/most\\_downloaded](http://pof.aip.org/features/most_downloaded)

Information for Authors: <http://pof.aip.org/authors>

### ADVERTISEMENT



**Running in Circles Looking  
for the Best Science Job?**

Search hundreds of exciting  
new jobs each month!

<http://careers.physicstoday.org/jobs>

physicstodayJOBS



## Relevance of the Thorpe length scale in stably stratified turbulence

Benjamin D. Mater, Simon M. Schaad, and Subhas Karan Venayagamoorthy<sup>a)</sup>

*Department of Civil and Environmental Engineering, Colorado State University, Fort Collins, Colorado 80523-1372, USA*

(Received 22 January 2013; accepted 6 June 2013; published online 22 July 2013)

Direct numerical simulations of stably stratified turbulence are used to compare the Thorpe overturn length scale,  $L_T$ , with other length scales of the flow that can be constructed from large-scale quantities fundamental to shear-free, stratified turbulence. Quantities considered are the turbulent kinetic energy,  $k$ , its dissipation rate,  $\epsilon$ , and the buoyancy frequency,  $N$ . Fundamental length scales are then the Ozmidov length scale,  $L_O$ , the isotropic large scale,  $L_{k\epsilon}$ , and a kinetic energy length scale,  $L_{kN}$ . Behavior of all three fundamental scales, relative to  $L_T$ , is shown to be a function of the buoyancy strength parameter  $NT_L$ , where  $T_L = k/\epsilon$  is the turbulence time scale. When buoyancy effects are dominant (i.e., for  $NT_L > 1$ ),  $L_T$  is shown to be linearly correlated with  $L_{kN}$  and not with  $L_O$  as is commonly assumed for oceanic flows. Agreement between  $L_O$  and  $L_T$  is only observed when the buoyancy and turbulence time scales are approximately equal (i.e., for the critical case when  $NT_L \approx 1$ ). The relative lack of agreement between  $L_T$  and  $L_O$  in strongly stratified flows is likely due to anisotropy at the outer scales of the flow where the energy transfer rate differs from  $\epsilon$ . The key finding of this work is that observable overturns in strongly stratified flows are more reflective of  $k$  than  $\epsilon$ . In the context of oceanic observations, this implies that inference of  $k$ , rather than  $\epsilon$ , from measurements of  $L_T$  is fundamentally correct when  $NT_L \approx 1$  and most appropriate when  $NT_L > 1$ . Furthermore, we show that for  $NT_L < 1$ ,  $L_T$  is linearly correlated with  $L_{k\epsilon}$  when mean shear is absent. © 2013 AIP Publishing LLC. [<http://dx.doi.org/10.1063/1.4813809>]

### I. INTRODUCTION

A relatively simple and objective measure of large-scale vertical overturns in turbulent oceanic flows is the Thorpe length scale,  $L_T$ .<sup>1</sup> Beyond its ability to indicate vertical eddy size from density profiles, however,  $L_T$  is of limited use in more fully characterizing turbulence unless some relationship with fundamental quantities of the flow can be determined. In stably stratified turbulence, these fundamental quantities include turbulent kinetic energy,  $k$ , dissipation rate of turbulent kinetic energy,  $\epsilon$ , buoyancy frequency,  $N$ , mean shear rate  $S$ , and molecular kinematic viscosity,  $\nu$ . Dougherty<sup>2</sup> and Ozmidov<sup>3</sup> originally suggested the length scale constructed from  $\epsilon$  and  $N$  should indicate the size of the largest eddy unaffected by buoyancy in stratified turbulence — this, of course being the well-known Ozmidov length scale,  $L_O = (\epsilon/N^3)^{1/2}$ . Subsequent interpretations of this early work popularized  $L_O$  as an outer limit on eddy size for a given level of turbulence, as reflected by  $\epsilon$ , acting against a stably stratified background density profile, reflected in  $N$ , and thus should be related to  $L_T$  (e.g., see Refs. 1 and 4). In this light,  $L_O$  has become the preferred fundamental counterpart to the directly measured  $L_T$  and, therefore, often serves as the critical link between a relatively unsophisticated observation and a fundamental aspect of turbulence as embodied in  $\epsilon$ .

Reliance on a common scaling between  $L_O$  and  $L_T$  is commonplace in the field of oceanography where direct measurement of  $\epsilon$  with microstructure profilers is far more difficult than that of density

<sup>a)</sup>E-mail: [vsakaran@colostate.edu](mailto:vsakaran@colostate.edu)

profiles from standard Conductivity, Temperature, Depth (CTD) profilers needed for calculation of  $N$  and  $L_T$  (see e.g., Refs. 4 and 5). Accurate inferences of  $\epsilon$  from vertical density profiles, however, inherently require dissipation at small scales to be in phase with the observed large scale motions at the instant of sampling. In other words, the outer scales of the flow must be directly determining the rate of dissipation at the smallest scales. In this study, we use direct numerical simulations (DNS) of decaying stably stratified turbulence and physical reasoning to argue that this commonly held assumption is only valid for the special case when turbulence and buoyancy time scales are approximately equal, i.e.,  $NT_L \approx 1$ , where  $T_L = k/\epsilon$  is the turbulence time scale or turbulence decay time. We can refer to this as the critical case since the turbulent Froude number (discussed later) which is simply given by  $(NT_L)^{-1}$  is approximately unity. For flows strongly influenced by buoyancy (i.e.,  $NT_L > 1$ ), we argue that an overturn size more truly reflects the instantaneous turbulent kinetic energy and show that  $L_T$  more generally agrees with a length scale constructed from this quantity,  $L_{kN} = (k/N^2)^{1/2}$ . In such cases, the outer scales of the flow are larger than the scale of buoyancy control as set by  $L_O$  and, instead, are strongly anisotropic and decoupled from  $\epsilon$ .

In what follows, we provide a brief discussion of the physical interpretations of the fundamental length scales, describe the generation and sampling of numerical data, and explicitly show the performance of various fundamental length scales in predicting  $L_T$  under different levels of stratification. We conclude with a discussion of the theoretical and practical implications of predicting  $k$  from measured Thorpe scales and consider our results in the context of other DNS, laboratory, and field studies.

## II. RELEVANT LENGTH AND TIME SCALES

Here, we discuss the calculation of the Thorpe scale and the physical interpretations of  $L_O$  and other fundamental length scales commonly used to describe stratified turbulence. By combining  $k$ ,  $\epsilon$ ,  $N$ ,  $S$ , and  $\nu$ , two at a time, one can easily construct nine length scales through dimensional analysis. Because we are only concerned with large-scale motions at sufficiently high Reynolds number, we assume that molecular effects are negligible and, thus, consider only those five length scales that exclude  $\nu$ .

### A. Thorpe length scale

The Thorpe scale can be calculated from an observed instantaneous density profile, such as that provided by CTD measurements in the field. Discrete density measurements from the instantaneous profile are monotonically sorted to give a gravitationally stable profile. The vertical distance a sample must be moved adiabatically in this process is its Thorpe displacement,  $\delta_T$ . For the vertical region of interest (e.g., the vertical extent of the DNS domain or, in an oceanic setting, the depths just encompassing a turbulent patch), the Thorpe scale is then calculated as the root-mean-square (rms)  $\delta_T$  for that region given by

$$L_T = \langle \delta_T^2 \rangle^{1/2}. \quad (1)$$

For a more thorough explanation of this process, see Ref. 1. Further details are also given in Sec. III.

A closely related measure of overturning is the Ellison length scale, defined as

$$L_E = \frac{\langle \rho'^2 \rangle^{1/2}}{|\partial \bar{\rho} / \partial z|}, \quad (2)$$

where  $\rho'$  is the turbulent density fluctuation about some mean background density,  $\bar{\rho}$ .  $L_E$  may be thought of as a statistical measure of the vertical distance traveled by fluid parcels before returning toward an equilibrium position or irreversibly mixing with surrounding fluid.<sup>6</sup> For the case when the sorted density profile exhibits a uniform gradient and  $\langle \rangle$  represents a vertical ensemble averaging applied to both  $\rho'^2$  and  $\delta_T^2$ ,  $L_E$  is exactly equal to  $L_T$ . Agreement between  $L_E$  and  $L_T$  was confirmed in the grid tow experiments of Itsweire<sup>7</sup> and the DNS of Itsweire *et al.*<sup>8</sup> for all but the most strongly stratified flows. In the runs with highest stratification, it was correctly proposed that  $L_E$  became larger than  $L_T$  due to the effects of internal gravity waves, despite relatively uniform background (i.e., sorted) density gradients. This may be attributed to differences in the averaging schemes used

for  $\langle \rho'^2 \rangle$  and  $\langle \delta_T^2 \rangle$  in the calculation of  $L_E$  and  $L_T$ , respectively. Specifically,  $\rho'^2$  was averaged over both vertical and lateral (i.e., temporal under Taylor's hypothesis) extents, while  $\delta_T^2$  was averaged only in the vertical. A lateral component of ensemble averaging in the presence of internal waves will tend to increase  $\langle \rho'^2 \rangle$ , and thus  $L_E$ , from what would be expected from a vertical ensemble alone. Thus,  $L_E$  can be biased toward larger values due to non-overturning wave motions, while  $L_T$  is free of reversible motions and, therefore, truly reflects vertical overturns. The bias increases with stratification as internal waves become more prominent relative to overturns. We use the traditional three-dimensional averaging scheme to calculate  $L_E$ , then use the comparison between  $L_T$  and  $L_E$  as an indicator of internal wave intensity in the present simulations.

## B. Fundamental scales

Dimensionally, five length scales can be constructed from  $k$ ,  $\epsilon$ ,  $N$ , and  $S$ . Those most common in literature include the turbulent length scale,  $L_{k\epsilon} = k^{3/2}/\epsilon$ ,<sup>9</sup> the Ozmidov length scale,  $L_O = (\epsilon/N^3)^{1/2}$ ,<sup>3</sup> and the Corrsin length scale,  $L_C = (\epsilon/S^3)^{1/2}$ .<sup>10</sup> The remaining two link turbulent kinetic energy to buoyancy frequency and mean shear are respectively:  $L_{kN} = (k/N^2)^{1/2}$  and  $L_{kS} = (k/S^2)^{1/2}$ .

Physically, the turbulent length scale,  $L_{k\epsilon}$ , can be thought to represent the largest eddies present in a flow when the effects of shear or buoyancy are negligible (i.e., isotropic turbulence). This interpretation assumes that such eddies are characterized by the velocity scale,  $k^{1/2}$ , and inertially transfer kinetic energy to smaller scales at a rate equal to  $\epsilon$ . The latter assumption stems from the second similarity hypothesis of Kolmogorov<sup>11</sup> and implies that  $L_{k\epsilon}$  should be a measure of the large-scale extent of the inertial subrange given truly isotropic flow.

When mean shear or stratification are not negligible, large-scale motions become increasingly anisotropic and have length scales that depart from the isotropic prediction of  $L_{k\epsilon}$ . The validity of Kolmogorov's hypothesis and the inertial subrange are then relegated to length scales smaller than  $L_O$  or  $L_C$  for buoyancy or shear-dominated flow, respectively. The largest eddy for which  $\epsilon$  is a valid estimate of down-scale energy transfer is then  $L_O$  when  $Ri_g > Ri_{g,c}$  or  $L_C$  when  $Ri_g < Ri_{g,c}$ , where  $Ri_{g,c}$  is some critical value of the gradient Richardson number,  $Ri_g = N^2/S^2$ , that delineates the two regimes. The associated velocity scales are  $(\epsilon/N)^{1/2}$  and  $(\epsilon/S)^{1/2}$ .

Physical interpretations of the final two fundamental length scales need not rely on any assumptions about the transfer rate of turbulent kinetic energy to smaller scales and, therefore, are not concerned with  $\epsilon$ . Rather, the focus remains on  $k$ . The only argument needed to bring physical significance to these scales is that their characteristic velocities are set by  $k^{1/2}$  with corresponding time scales given by  $N^{-1}$  and  $S^{-1}$ , respectively. In this sense,  $L_{kN}$  and  $L_{kS}$  more generally describe large-scale motions in their respective regimes of buoyancy- and shear-dominated flows than their counterparts  $L_O$  and  $L_C$ .

In this study, we focus on buoyancy-dominated turbulence that is free of shear and, therefore, will emphasize the roles played by  $L_O$  and  $L_{kN}$  in describing overturning motions. Considering the fundamental quantities of interest, the dimensionless parameters needed to characterize such flows are the turbulent Reynolds number,  $Re_L = k^2/\epsilon\nu$ , and the turbulent Froude number,  $Fr_k = \epsilon/(Nk)$ . If one considers the turbulent time scale,  $T_L$ , the Froude number may be rewritten as  $Fr_k = (NT_L)^{-1}$ . This alternative formulation explicitly represents the competition of inertial and buoyancy time scales; therefore, we choose to make reference to  $NT_L$ , rather than  $Fr_k$ , throughout this paper. When  $NT_L > 1$ , motions due to gravitational perturbations occur rapidly (i.e., on a short time scale) relative to inertial motions of existing turbulence. Thus, we will classify this as a "subcritical" regime (i.e., buoyancy effects are strong). Conversely, flow regimes with  $NT_L < 1$  will be classified as "supercritical" (i.e., buoyancy effects are weak). In this state, it is the inertial motions that are rapid and, thus, act to mitigate the motions from the slower gravitational instabilities.

It can easily be shown that  $L_{kN}/L_O = (NT_L)^{1/2}$ . Furthermore,  $NT_L$  links these two buoyancy scales to the isotropic large scale:  $L_{k\epsilon}/L_{kN} = NT_L$ , and thus,  $L_{k\epsilon}/L_O = (NT_L)^{3/2}$ . For  $NT_L > 1$ , this implies that  $L_{k\epsilon} > L_{kN} > L_O$ . For the special case of "critical" flow,  $NT_L = 1$ , all the three length scales equate.

The turbulent Reynolds number indicates the competition of inertial and viscous forces in the flow and provides a measure of the range of scales present. The latter interpretation is strictly valid

for isotropic flow and follows from  $Re_L = k^2/\epsilon v = (L_{k\epsilon}/\eta)^{4/3}$ , where  $\eta = (\nu^3/\epsilon)^{1/4}$  is the Kolmogorov length scale. When buoyancy introduces anisotropy, the large scales are limited to values less than the isotropic potential expressed in  $L_{k\epsilon}$ . What the actual outer scale is remains to be seen and is the subject of the current work.

While  $NT_L$  and  $Re_L$  are the only parameters needed to fully characterize a purely stratified flow on dimensional grounds, a third parameter that frequently appears in literature is the buoyancy Reynolds number or “activity parameter”,  $Re_b = \epsilon/(\nu N^2)$  (see e.g., Refs. 12–14), which may be interpreted as a relative measure of turbulent stirring (i.e., inertia) to combined stabilizing effects from buoyancy and viscosity.<sup>15</sup> The utility of this parameter is limited by the inherent ambiguity elucidated in this interpretation. For example, an increase in  $Re_b$  could represent increased inertial effects relative to viscosity (increased  $Re_L$ ) just as it could represent increased inertial effects relative to buoyancy (decreased  $NT_L$ ). This becomes clear when formulating the activity parameter in terms of its more fundamental constituents, i.e.,  $Re_b = Re_L(NT_L)^{-2}$ . When parameterizing aspects of the flow (e.g., mixing efficiency) on  $Re_b$  alone, care should be taken to ensure that observed trends are not dependent on trajectory through an  $NT_L - Re_L$  parameter space. Otherwise,  $Re_b$ -based parameterizations should be qualified with accompanying valid ranges of  $Re_L$  and/or  $NT_L$ .

The activity parameter may be written as  $Re_b = (L_O/\eta)^{4/3}$ , and thus also indicates the range of scales free from the anisotropic effects of buoyancy. It follows that  $Re_b$  describes the full range of turbulent scales only in the special case that  $L_O$  coincides with the largest scale of the flow. Obviously,  $Re_b$  loses significance (from a physical standpoint) for weakly stratified turbulence ( $N \rightarrow 0$ ) in which  $L_O$  far exceeds outer dimensions of the flow.

### III. NUMERICAL APPROACH

#### A. Set up

Direct numerical simulations (DNS) were used to simulate decaying homogeneous stably stratified turbulence without further production (i.e., shear-free turbulence). This idealized condition is akin to a breaking internal gravity wave or other intermittent disturbance leading to turbulence that is isolated from boundaries and free of sustained mean shear. The laboratory equivalent is the grid-tow experiment in which a bi-lateral mesh is towed through a stratified bath.

The numerical simulations performed for this study were carried out using the pseudo-spectral code developed by Riley *et al.*<sup>16</sup> This code simulates a flow field that is periodic in all three spatial directions, with a constant background density gradient (since the flow is homogeneous) with a buoyancy frequency  $N^2 = (-g/\rho_0)(\partial\bar{\rho}/\partial z)$  (see Refs. 16 and 17 for further details). The turbulence is initialized as a Gaussian, isotropic, and solenoidal field with initial length and velocity scales  $L_0$  and  $u_0$ , respectively. The flow domain is a cube with dimensions  $\mathcal{L} = 2\pi$  with a  $256^3$  grid-point resolution. After the first eddy turnover period,  $1L_0/u_0$ , the dissipation peaks and begins to decay. We interpret this as a signature of fully developed turbulence. Prior to this time, the statistics are not representative of decaying stratified turbulence and, thus, these initial transients were ignored in this study. The duration of all simulations was  $5L_0/u_0$ .

#### B. Parameter values

The strength of stratification can be characterized by an initial Richardson number defined as  $Ri_0 = (NL_0/u_0)^2$ . To more specifically investigate temporal variance in flow characteristics, however, we must turn to  $NT_L$ . For this work, seven DNS runs were performed with  $Ri_0$  varying from 0.01 to 158. The Prandtl number  $Pr = \nu/\kappa = 1$  in order to ensure accurate resolution of the smallest scales of the density field. During the runs,  $Re_L$  varied narrowly around  $O(10^3)$ , and  $NT_L$  varied from  $O(10^{-1})$  to  $O(10^2)$ . The peak value of  $Re_b$  varied from  $O(10^0)$  to  $O(10^5)$ .

Using DNS of slightly lower  $Re_L$  values ( $O(10^1)$  to  $O(10^3)$ ) and a narrower range in  $NT_L$  ( $O(10^0)$  to  $O(10^1)$ ), Shih *et al.*<sup>13</sup> showed that flows could be categorized into three distinct  $Re_b$ -regimes based on the behavior of mixing efficiency: a “diffusive” regime where  $\epsilon/(\nu N^2) < 7$ , an “intermediate” regime where  $7 < \epsilon/(\nu N^2) < 100$ , and an “energetic” regime where  $\epsilon/(\nu N^2) > 100$ . Because of the

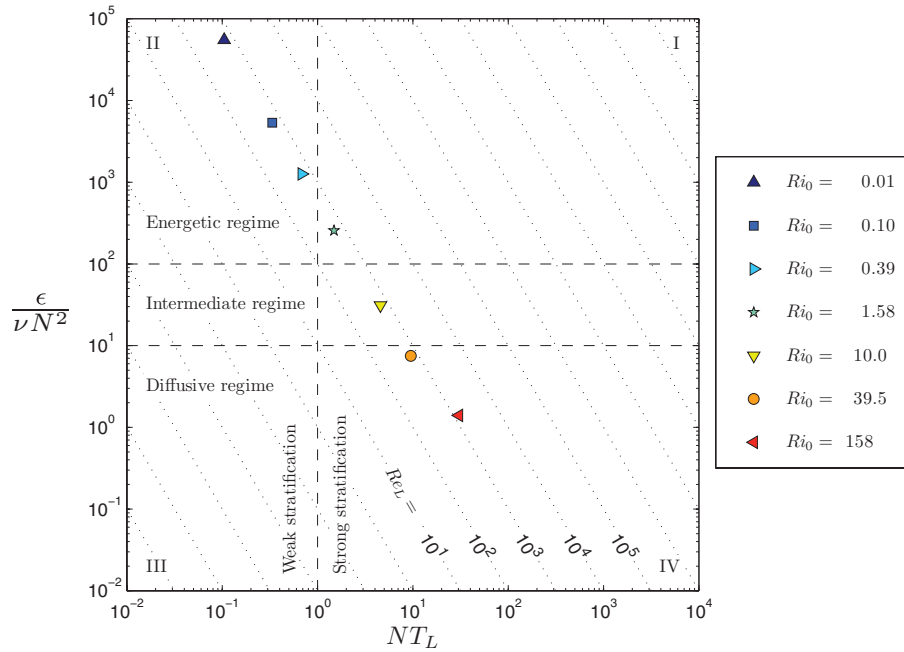


FIG. 1. Peak  $Re_b$  ( $\epsilon/(\nu N^2)$ ) values and corresponding  $NT_L$  values plotted over  $Re_b$  regimes by Shih *et al.*<sup>13</sup> and  $NT_L$  regimes reported in the current study.

aforementioned ambiguity in  $Re_b$ , the universality of these regime limits remains uncertain (e.g., if mixing efficiency were to become independent of viscosity in high  $Re_L$  flows typical of the ocean, the intermediate-energetic transition would shift to higher values of  $Re_b$ ). Nonetheless, we can conceptualize the turbulent state of the current simulations according to the regimes of Shih *et al.*<sup>13</sup> and the stratification parameter  $NT_L$ .

Turbulent regimes are illustrated in Figure 1 where a line at  $NT_L = 1$  has been included to tentatively delineate weak ( $NT_L < 1$ ) and strong ( $NT_L > 1$ ) stratification. Recall, weak stratification implies flows that are not affected by buoyancy forces and in the context of these simulations are more or less isotropic, while the converse is true for strong stratification. Quadrant I represents strongly stratified flows at high values of  $Re_L$ . Flows in this quadrant are energetic while at the same time influenced by buoyancy forces. This regime characterizes geophysical flows. Quadrant II represents flows that are energetic but the stratification is weak. In the limit of zero stratification, this regime marks the classical isotropic turbulence limit. Flows in quadrant III are characterized by low  $Re_L$  and are considered “diffusive” in that transport of both momentum and scalar occurs dominantly through molecular diffusion as the laminar limit is approached. Flows in quadrant IV are also characterized as “diffusive,” despite higher  $Re_L$  values, due to the suppression of turbulence by strong buoyancy effects. The ultimate quest is to understand the physics of strongly stratified energetic flows as denoted by quadrant I. Data points for the current study are barely in the lower end of this range.

### C. Thorpe sorting

As discussed in Sec. II A, the Thorpe scale is calculated by adiabatically sorting density profiles for gravitational stability. Following Smyth and Moum,<sup>18</sup> there are two alternative sorting techniques: density is known for all points  $(x, y, z)$  in the domain, therefore, we are free to sort values for one-dimensional profiles at each  $(x, y)$  or sort the entire domain in a three-dimensional sense as was suggested by Winters *et al.*<sup>19</sup>

One-dimensional sorting provides profile-based displacements,  $\delta_T = (z - z_{sort})$  for each grid point, where  $z_{sort}$  is the depth at which a fluid parcel originating from depth  $z$  would be gravitationally

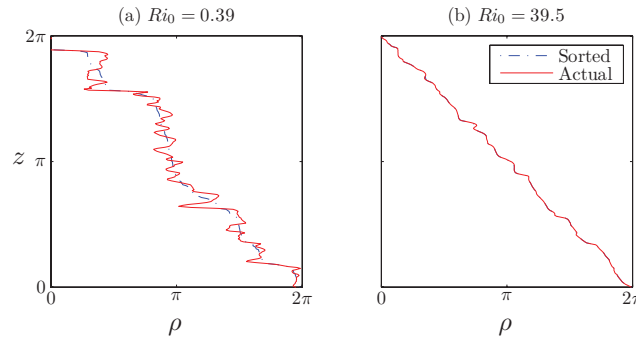


FIG. 2. Instantaneous and sorted density profiles for (a) moderate and (b) strong stratification.

stable within a given profile. Typical instantaneous and stable density profiles are plotted in Figure 2 for two different strengths of stratification. This figure also illustrates the homogeneous nature of the turbulence and the lack of coherent turbulent patches typical of shear layers, etc. Thus, we are not concerned with identifying vertical regions for Thorpe scale calculations as was done by Smyth *et al.*<sup>20</sup> Instead, we treat the entire domain as one turbulent patch. Periodic boundary conditions allow for inclusion of all grid points in these calculations.

In three-dimensional sorting, a fluid parcel is moved to a stable depth relative to all vertical and lateral neighbors and associated with a displacement  $\delta_{T3D} = (z - z_{sort3D})$ , where  $z_{sort3D}$  is the gravitationally stable depth if sorting is also monotonic in the lateral directions (i.e., lateral density gradients are also minimized); thus a parcel's stable position is not necessarily directly above or below its point of origin. Isopycnal planes of the sorted flow field will be free of internal wave crenulations — the same cannot be said for the isopycnals resulting from one-dimensional sorting.

Once sorting has been performed, the Thorpe scale can be calculated as the rms of either displacement set. Here we distinguish one-dimensional and three-dimensional values as  $L_T$  and  $L_{T3D}$ , respectively. Because  $\delta_{T3D}$  can be influenced by non-overturning wave motions (through allowing fluid parcels to be “moved” laterally),  $L_{T3D}$  provides a measure of general scalar fluctuations. In contrast,  $L_T$  is a specific measure of unstable overturning. As such,  $L_T < L_{T3D}$  when internal waves are significant.<sup>18</sup> The one-dimensional and three-dimensional Thorpe scales are compared in Figure 3(a). Wave effects appear minimal, even for very stable simulations. An objective of this work is to present practically relevant data to the oceanography community in which field sampling is more analogous to the methods leading to the one-dimensional Thorpe scale. Considering this, and the relatively good agreement between  $L_T$  and  $L_{T3D}$ , we will refer exclusively to  $L_T$  in the rest of this paper.

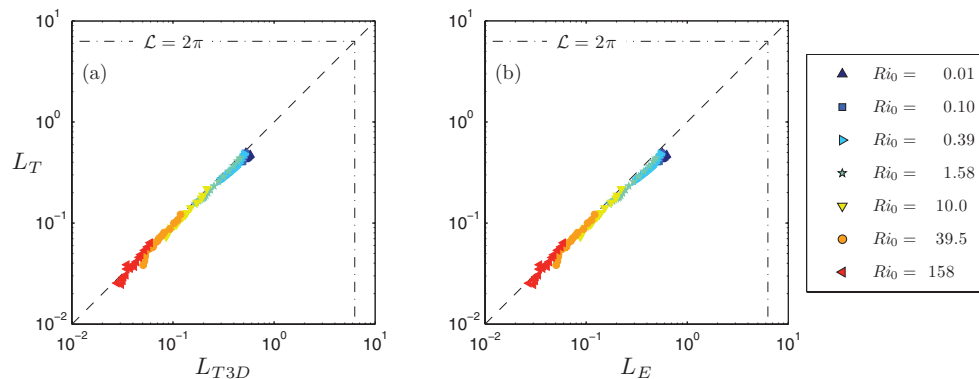


FIG. 3. One-dimensional Thorpe scale,  $L_T$ , versus (a) three-dimensional Thorpe scale,  $L_{T3D}$ , and (b) Ellison length scale,  $L_E$ . Computational domain extents are indicated by dash-dotted line.

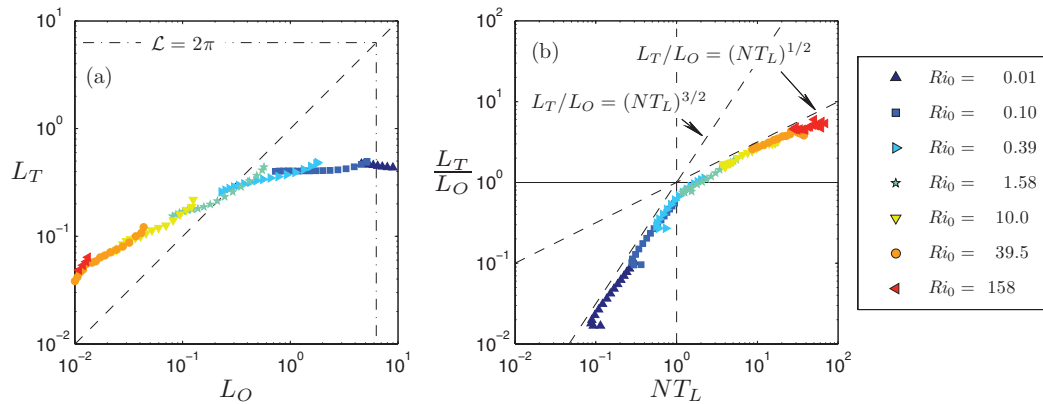


FIG. 4. Ozmidov length scale,  $L_O$ , versus Thorpe scale,  $L_T$ : (a) direct comparison, and (b) plotted against the dimensionless stratification parameter,  $NT_L$ .

## IV. DNS RESULTS

### A. Thorpe vs. Ellison scales

Prior to investigating fundamental length scales, we first focus on the correlation between the Ellison and Thorpe length scales as a simple check on the nature of the overturns. Figure 3(b) shows excellent agreement between  $L_E$  and  $L_T$ . The density fluctuations due to non-overturning internal waves appear to be of minimal influence on  $L_E$  (see Figure 3(a)).

### B. Thorpe vs. Ozmidov scales

Following the work of Dillon,<sup>4</sup> the Thorpe scale,  $L_T$ , has become a popular predictor of the Ozmidov scale,  $L_O$  (or vice versa). Field observations and laboratory experiments imply a linear dependency of the form  $L_O = \alpha L_T$  with common estimates of  $\alpha$  agreeing with Dillon's value of 0.8.<sup>7,21</sup> DNS of stratified turbulence have also revealed correlation between  $L_O$  and  $L_T$ , but indicate the relationship is nonlinear and perhaps a function of the gradient Richardson number,  $Ri_g$ , (see e.g., Ref. 8) or a function of overturn age in the case of a shear layer with Kelvin-Helmholtz billows (see Refs. 18 and 20). As shown in Figure 4(a), we too find a nonlinear dependency between the two length scales for our shear-free simulations. Since the current simulations effectively lack mean shear, the appropriate non-dimensional parameter to further investigate this trend with is  $NT_L$  (rather than  $Ri_g$ ). Hypothetically, one could also investigate Reynolds number effects; however, the current study is limited to a single order of magnitude range in  $Re_L$  (i.e.,  $O(10^3)$ ). As such, we implicitly assume Reynolds number independence in the remainder of this discussion.

In Figure 4(b), we see a clear dependence of  $L_T/L_O$  on  $NT_L$  over possibly two regimes delineated by  $NT_L \approx 1$ . In the weakly stratified regime ( $NT_L < 1$ ), the size of observed overturns is less than  $L_O$ , theoretically indicating negligible influence of buoyancy at the outer scales of the flow. At the regime break  $L_O$  becomes smaller than the overturn size, and here we expect an onset of buoyancy control. While the general slope of the data points does decrease in the strongly stratified regime ( $NT_L > 1$ ), it does not completely flatten nor does the ratio of scales go to unity. Thus, contrary to common assertions, the Ozmidov scale does not appear to be the limiting size of overturns in strongly stratified turbulence except for the special case of  $NT_L \approx 1$ . Beyond this regime break, overturn size continues to increase beyond  $L_O$  as a function of  $NT_L$ .

### C. Thorpe vs. turbulent kinetic energy scale

Next, we investigate  $L_{kN}$  as an alternative predictor of  $L_T$ . Direct comparison is shown in Figure 5(a). Unlike the Ozmidov scale,  $L_{kN}$  shows a strongly linear trend with  $L_T$  through all but the three runs with lowest  $Ri_0$ . Further investigation of  $NT_L$  dependency is shown in Figure 5(b). Again,

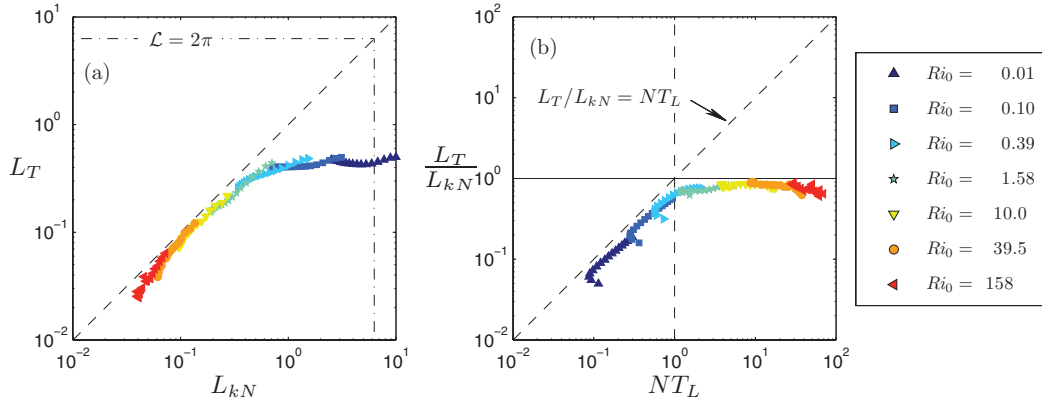


FIG. 5. Kinetic energy length scale,  $L_{kN}$ , versus Thorpe scale,  $L_T$ : (a) direct comparison, and (b) plotted against the dimensionless stratification parameter,  $NT_L$ .

two regimes delineated by  $NT_L \approx 1$  are apparent, and  $L_T$  is less than the buoyancy-dependent scale in the weakly stratified regime. The ratio,  $L_T/L_{kN}$ , however, reaches a constant near unity for the strongly stratified regime. It appears, then, that  $L_{kN}$  is a better indicator of overturning events than  $L_O$  in buoyancy dominated stratified turbulence ( $NT_L > 1$ ). Referring back to Figure 4(b), this result is reflected in  $L_T/L_O$  data closely following the line of  $(NT_L)^{1/2}$  for  $NT_L > 1$  (cf.  $L_{kN}/L_O = (NT_L)^{1/2}$ ).

#### D. Thorpe vs. isotropic large scale

Finally,  $L_T$  is compared with the isotropic large scale,  $L_{k\epsilon}$ , for the main purpose of investigating their relationship in the weakly stratified regime. Direct comparison is given in Figure 6(a). Clearly,  $L_{k\epsilon}$  overestimates  $L_T$  in runs of strong stratification, and the discrepancy increases with  $Ri_0$ . In this regime, Figure 6(b) shows that  $L_T/L_{k\epsilon}$  data closely follow the line of  $(NT_L)^{-1}$ . This is a direct result of  $L_T \sim L_{kN}$  for  $NT_L > 1$  (cf.  $L_{k\epsilon}/L_{kN} = NT_L$ ). Only for weakly stratified runs does there appear to be close correlation. Agreement in the weakly stratified regime is clearly shown in Figure 6(b), where for  $NT_L < 1$ , the ratio is near unity.

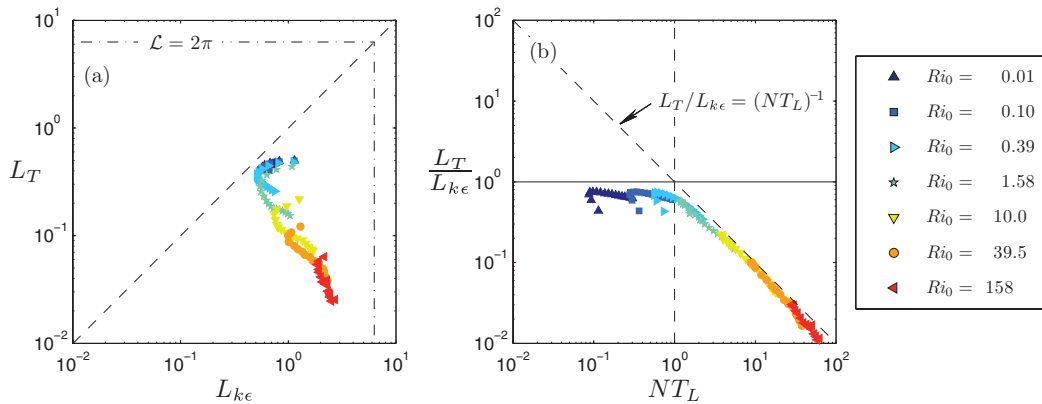


FIG. 6. Kinetic energy isotropic length scale,  $L_{k\epsilon}$ , versus Thorpe scale,  $L_T$ : (a) direct comparison, and (b) plotted against the dimensionless stratification parameter,  $NT_L$ .

## V. DISCUSSION

### A. Physical interpretations

For strongly stratified turbulence, the lack of correlation between  $L_T$  and  $L_O$  implies that the rate of dissipation,  $\epsilon$ , is not fundamental in describing the outer scales of the flow. It should not necessarily come as a surprise that  $\epsilon$  under-performs in this regard. Recall, the seminal works of Dougherty<sup>2</sup> and Ozmidov<sup>3</sup> sought not to determine the outer scale of the flow, but rather to define the largest scale that could remain isotropic in the presence of buoyancy forces (i.e., the large-scale extent of the inertial subrange). This early theory is entirely compatible with the possibility of anisotropic overturns larger than  $L_O$  in strongly stratified flows. Such eddies would exist at scales larger than those of the inertial subrange and transfer energy to other scales at rates different than  $\epsilon$ . In other words, these eddies do not adhere to the second similarity hypothesis of Kolmogorov and, as such, do not have a form determined by  $\epsilon$ .

Instead, the outer scales of strongly stratified turbulence are more indicative of the total turbulent kinetic energy,  $k$ , as implied by the linear relationship between  $L_T$  and  $L_{kN}$  for  $NT_L > 1$ . This essentially validates the physical reasoning that the time scale of these eddies scales with  $N^{-1}$ , and the velocity goes unequivocally with  $k^{1/2}$ , not  $(\epsilon/N)^{1/2}$ . In order for these eddies to exist,  $N^{-1}$  must be shorter than the turbulent decay time,  $T_L$  (i.e., anisotropic eddies larger than  $L_O$  cannot exist if turbulence decays quicker than the eddy can turn over).

In the weakly stratified regime where  $NT_L < 1$ , the lack of correlation between  $L_T$  and  $L_O$  is due to the negligible influence of buoyancy. In other words, the flow is nearly isotropic at all scales and the time scale of the largest eddies is much shorter than  $N^{-1}$ . Instead, even the large eddies are associated with length and time scales dependent on  $\epsilon$  — these, of course, being  $L_{k\epsilon}$  and  $T_L$ , respectively. It is important to note that this would only be the case in flows free of mean shear or the influences of boundaries. The influence of shear or boundaries could induce anisotropic motions even when  $NT_L < 1$ .

### B. Implications

The linear relationship between  $L_T$  and  $L_{kN}$  has both practical and theoretical implications. An important theoretical implication of a linear relationship between  $L_T$  and  $L_{kN}$  is that the ratio of the turbulent potential to the turbulent kinetic energy is likely a constant value in strongly stratified turbulence, where the turbulent potential energy is  $E_p = -(g/\rho_0)\langle\rho'^2\rangle/(2\partial\bar{\rho}/\partial z)$ . This is a direct implication of  $L_E \sim L_T \sim L_{kN}$ . From the definition of the Ellison length scale, the turbulent potential energy can be rewritten as  $E_p = N^2 L_E^2/2$ . Similarly, from the definition of  $L_{kN}$ , the turbulent kinetic energy can be written as  $k = N^2 L_{kN}^2$ . Taking the ratio, we see that  $E_p/k = (L_E/L_{kN})^2/2$ . Assuming the conditions for  $L_E \sim L_T$  are valid (i.e., internal wave effects are minimal) and  $NT_L > 1$ , our results imply that  $E_p/k \approx 1/2$ . This result is confirmed in Figure 7 for the cases of strong stratification.

For weak stratification, the relationship,  $L_T \sim L_{k\epsilon}$ , gives  $k \sim (\epsilon L_T)^{2/3}$ . This is in agreement with the theory of Luketina and Imberger<sup>22</sup> and later shown to hold for energetic stages of grid turbulence in various laboratory settings by Ivey and Imberger.<sup>23</sup> In this regime, the ratio of potential to kinetic energy becomes  $E_p/k = N^2 \epsilon^{-2/3} (L_E/L_{k\epsilon}^{1/3})^2/2$ , or  $E_p/k \sim N^2 \epsilon^{-2/3} L_T^{4/3}/2$ . Clearly then, energy partitioning is not given by a simple constant when  $NT_L < 1$ .

The most obvious implication of  $L_T \sim L_{kN}$  for  $NT_L > 1$  from a practical standpoint is the resulting ability to infer turbulent kinetic energy from observed overturns in a density profile. This would preclude the need for high resolution measurements of three-dimensional velocity fluctuations and, instead, require only the use of a CTD profiler. It is important to note that this fundamentally differs from the common practice of inferring dissipation from density profiles using the assumption of  $L_T \sim L_O$  — dissipation must still be measured from microstructure profiling if  $N$  and  $T_L$  are not equal. If microstructure measurements are available and are collected simultaneously with density measurements, then estimates of both  $k$  and  $\epsilon$  can be obtained. In turn, the dimensionless parameters,  $NT_L$  and  $Re_L$ , can be calculated. Access to  $NT_L$  and  $Re_L$  provides a more insightful description of the flow than that provided by the commonly used “activity parameter”,  $Re_b$ , under the reasoning stated in Sec. II B.

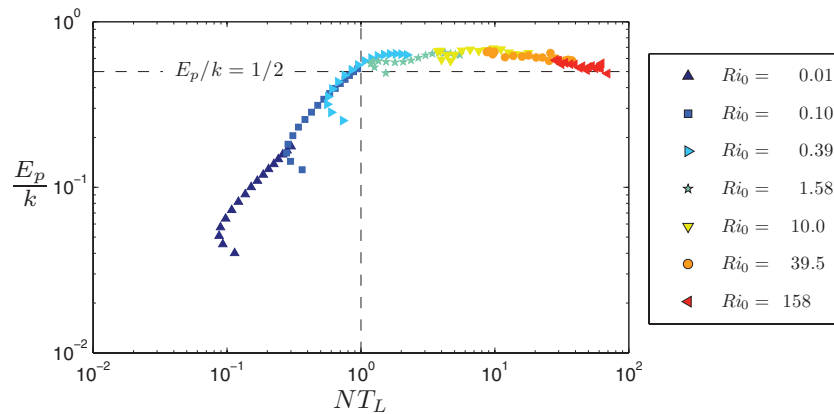


FIG. 7. Ratio of turbulent potential energy  $E_p$  to turbulent kinetic energy  $k$  versus  $NT_L$ .

So far, we have considered shear-free flow. Inclusion of shear would necessitate an additional dimensionless parameter to fully characterize the flow. Through dimensional analysis this parameter can be shown to be  $ST_L = Sk/\epsilon$  or, alternatively,  $Ri_g$ . Now, the analysis is no longer cleanly restricted to two regimes based on  $NT_L$ , but rather a two-dimensional parameter space involving some paired combination of  $NT_L$ ,  $ST_L$ , and  $Ri_g$  as axes. This could be, for example, an  $Ri_g - NT_L$  parameter space. With this approach, the two previous  $NT_L$  regimes can each be subdivided into two  $Ri_g$ -based regimes (assuming a critical value of  $Ri_g$  exists for describing flow behavior and Reynolds number independence). While we find  $L_T \sim L_{kN}$  for  $NT_L > 1$  when shear is absent, the behavior likely changes for low values of  $Ri_g$  — even if  $NT_L$  remains high. Indeed, Venayagamoorthy and Stretch<sup>24</sup> used the shear-flow DNS of Shih *et al.*<sup>13</sup> to show that the overturning scale, as represented by  $L_E$ , correlates linearly with  $L_{kS}$ , rather than  $L_{kN}$ , when  $NT_L > 1$  and  $Ri_g < 0.25$ .

The applicability of our DNS results to turbulence in the open ocean is yet to be determined. To do so would require simultaneous measurements of density and the fundamental quantities from which the length scales of interest can be calculated. These, of course, being  $k$ ,  $\epsilon$ ,  $N$ , and  $S$ . Since non-stationarity and inhomogeneity exist in ocean turbulence, it would be ideal for all these quantities to be measured from a common sampler on a single cast. Herein lies a practical challenge to the technical oceanographic community. If overcoming this challenge were to indeed validate our findings, it would then be up to the investigator in the field to determine in which regime the flow of interest belongs. This, of course, would necessitate the calculation of perhaps  $NT_L$  and  $Ri_g$ . While  $Ri_g$  is a mean flow parameter that is relatively easy to obtain,  $NT_L$  includes  $k$  — the very quantity for which an inferred value is being sought. Because of the difficulty in directly measuring  $k$  and  $\epsilon$ , common values of  $NT_L$  — or more specifically the decay time,  $T_L$  — are not readily available for ocean turbulence. It is important to note, however, that the common practice of linearly relating Thorpe and Ozmidov scales implicitly assumes  $NT_L \approx 1$ . As the strength of stratification relative to  $T_L$  and  $S$  increases in the ocean, the error of assuming  $L_T \sim L_O$  increases, while that of  $L_T \sim L_{kN}$  remains valid (given common values in Reynolds number).

### C. Comparisons with previous studies

The study of Itsweire *et al.*<sup>25</sup> represents a laboratory-based analogue to the current work and, thus, warrants mention. In their experiments, turbulence was generated free of shear using a bilateral mesh and allowed to decay in the presence of stable stratification. As in the current simulations, the density gradient was initially uniform. Their data suggest that the buoyancy parameter,  $NT_L$ , is less than unity near the grid where turbulence is intense relative to buoyancy. The parameter then grows monotonically with distance from the grid (i.e., turbulence age) to values greater than unity as turbulence decays while buoyancy effects persist due to incomplete mixing of the ambient density gradient. The growth of  $NT_L$  is also observed in the current simulations where  $N$  remains

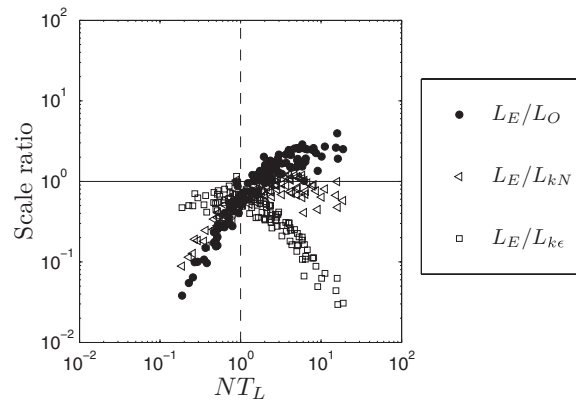


FIG. 8. Variation of  $L_E/L_O$  (circles),  $L_E/L_{kN}$  (triangles), and  $L_E/L_{k\epsilon}$  (squares) with  $NT_L$  for data of Itsweire *et al.*<sup>25</sup>

fixed. Length scale comparisons from their data are shown in Figure 8, where  $L_E$  is taken to be an approximation of  $L_T$ . In agreement with the current findings,  $L_E \sim L_{k\epsilon}$  when  $NT_L \lesssim 1$  (young turbulence proximal to grid), and that  $L_E \sim L_{kN}$  when  $NT_L \gtrsim 1$  (old turbulence distal to grid). The best agreement between  $L_O$  and  $L_E$  occurs just as the flow is transitioning between these two stages (i.e.,  $NT_L \approx 1$ ).

We now briefly compare our results with the shear-layer DNS of Smyth and Moum<sup>18</sup> and Smyth *et al.*<sup>20</sup> In their simulations, gradients in mean velocity and density are isolated to a finite layer within the flow that becomes turbulent via Kelvin-Helmholtz (K-H) instabilities that are thought to be frequent in the deep ocean. Following breakup of the pre-turbulent K-H billow, both scales are shown to decrease, with  $L_T$  decreasing most rapidly so that the ratio,  $L_O/L_T$ , increases nearly monotonically with time. This leads the authors to suggest that the ratio can be used as an “observational clock” of event age. Smyth *et al.*<sup>20</sup> also find that  $L_T$  is in fair agreement with the length scale,  $L_b = w_{rms}/N$  ( $\approx \sqrt{\frac{2}{3}}L_{kN}$ ), early and is in excellent agreement with  $L_{k\epsilon}$  late. Early correlation between  $L_T$  and  $L_b$  is also shown by Smyth and Moum<sup>18</sup> (larger values of their Figure 10(b)). These findings are suggestive that  $NT_L$  decreases with the age of K-H turbulence and, thereby, evolves in the opposite sense of the uniform-gradient case. Apparently, any increase in  $T_L$  as K-H turbulence decays is mitigated by reduced  $N$  as mixing takes place. Thus, the flow approaches the weakly stratified regime. In the current work and the experiments of Itsweire *et al.*,<sup>25</sup>  $N$  is constant or decreases minimally so that stratification becomes dominant as inertial motions decay. The growth of  $T_L$  for K-H turbulence may also be suppressed by some lingering production due to shear.

Smyth *et al.*<sup>20</sup> also highlight the effects of variation in Prandtl number. Their data suggest that length scale ratios become dependent on  $Pr$  late in the simulation if isotropy is assumed (e.g., if, say,  $L_{k\epsilon}$  is approximated by  $w_{rms}^3/\epsilon$ ). Interestingly, however, the dependence on  $Pr$  vanishes when the assumption of isotropy is lifted, and data from runs of high  $Pr$  collapse upon those for which  $Pr = 1$ . Runs of high  $Pr$  appear most affected by the assumption of isotropy, while the run with  $Pr = 1$  is relatively insensitive. This could be a Reynolds number effect; due to practical limitations on grid resolution, the high  $Pr$  runs are limited to low  $Re$ . At low  $Re$ , the vertical turbulent motions are more susceptible to dampening by buoyancy even if buoyancy effects are small (i.e.,  $NT_L \approx 1$ ). Hence, the isotropic assumption is less valid for runs of high  $Pr$  simply because  $Re$  is low.

In oceanic applications, Prandtl number is indeed greater than unity; however, the Reynolds number of these flows is also large so that turbulent advection dominates molecular diffusion of density and Prandtl number effects can often be neglected. The current work sacrifices high  $Pr$  for high  $Re$  with the hopes that the simulations are more representative of oceanic turbulence. This, of course, remains difficult to prove conclusively due to the practical limitations of DNS.

Finally, the data set of Moum<sup>26</sup> can be used to compare the current work to actual observations of deep-ocean turbulence. These observations indicate good agreement between  $L_T$ ,  $L_O$ , and  $L_b$  over

the range of turbulent patches chosen (i.e.,  $L_T \approx 1.1L_O$  and  $L_T \approx 1.0L_b$ ). The observed oceanic relation  $L_T \sim L_b$  is consistent with the present results. Moun's measurements of the ratio  $L_O/L_T$  vary by about half an order of magnitude, possibly consistent with our finding that this ratio varies with  $NT_L$ . Comparison with our Figure 4(b) suggests that  $NT_L$  varies between about 1/2 and 10 in the deep-ocean turbulent events observed in that study.

## VI. CONCLUSIONS

The utility of the Thorpe length scale,  $L_T$ , in describing the physics of stratified turbulence is dramatically increased when it can be related to a length scale constructed from fundamental quantities of the flow. In light of the findings here, Thorpe scales of decaying, shear-free stratified turbulence exhibit behavior belonging to one of two regimes defined by ranges in the stratification strength parameter,  $NT_L$ . This is applicable for the range of  $Re_L$  investigated. Our results show that  $L_T$  correlates closely with the fundamental length scales,  $L_{kN}$  and  $L_{k\epsilon}$ , in the cases of strong stratification ( $NT_L > 1$ ) and weak stratification ( $NT_L < 1$ ), respectively. In neither regime does  $L_T$  have a linear relationship with the Ozmidov scale,  $L_O$ ; only for the special case of  $NT_L \approx 1$  does  $L_O$  describe  $L_T$ .

The most obvious implication of the current study is that the utility of the Thorpe scale lies in its ability to indicate the turbulent kinetic energy, rather than the rate of its dissipation when stratification is relevant. This is of practical pertinence from the standpoint that  $k$  can be inferred using density profile measurements alone, whereas, accurate estimates of  $\epsilon$  must be obtained from more direct methods such as microstructure profiling. It should be noted that direct measurement of  $k$  is not trivial due to contamination by wave motions and hence the ability to infer  $k$  from density profile measurements will be a major breakthrough. When complemented by direct measurements of  $\epsilon$ , inferred values of  $k$  allow for the calculation of  $Re_L$  and  $NT_L$  — dimensionless parameters upon which aspects of the flow (e.g., mixing efficiency) can be parameterized. Such parameterizations may be more insightful than those based on the activity parameter,  $Re_b$ , which ambiguously combines the influences of  $Re_L$  and  $NT_L$  and is independent of  $k$ .

Despite our findings, there exists a long history of studies that find acceptable agreement between  $L_T$  and  $L_O$ . This is perhaps attributed to measured flows having values of  $NT_L$  close to unity. If this is indeed the case, the current findings support the common practice of inferring  $\epsilon$ . More importantly, the current findings suggest that  $k$  can also be inferred since  $L_O \sim L_{kN} \sim L_T$  when  $NT_L \approx 1$ . To verify this assertion and the general findings of this study, independent measurements of  $k$ ,  $\epsilon$ , and density profiles are required for high Reynolds number flows. Being able to make these measurements simultaneously and from the same sampler is ideal, yet not widely carried out due to technical challenges.

Finally, the results presented here are for shear-free flows. Inclusion of mean shear would necessitate consideration for an additional dimensionless parameter ( $ST_L$  or  $Ri_g$ ) to fully characterize the flow. Predicting the behavior of overturning in stratified shear-flow may, therefore, require consideration for regimes additional to those defined by  $NT_L$ . Despite this added complication, we predict that the outer scales of the flow will remain more linearly correlated with length scales constructed from  $k$  than those involving  $\epsilon$ , so long as the outer scales are sufficiently anisotropic.

## ACKNOWLEDGMENTS

The authors thank the two referees for their constructive comments and recommendations. S.K.V. wishes to thank Professor Derek Stretch for many insightful discussions on stratified turbulence and Professor Jim Riley for providing his DNS code. B.D.M. and S.K.V. gratefully acknowledge the support of the Office of Naval Research under Grant Nos. N00014-12-1-0282, N00014-10-1-0607, and N00014-12-1-0938 (Scientific officers: Dr. Terri Paluszkiwicz and Dr. Scott Harper). S.M.S. was supported by the National Science Foundation under Grant No. OCE-1151838.

<sup>1</sup> S. A. Thorpe, "Turbulence and mixing in a scottish loch," *Philos. Trans. R. Soc. London, Ser. A* **286**, 125–181 (1977).

<sup>2</sup> J. P. Dougherty, "The anisotropy of turbulence at the meteor level," in *Electron Density Profiles in the Ionosphere and Exosphere*, edited by B. Maehlum (MacMillan Company, Pergamon Press, 1962), p. 92.

- <sup>3</sup>R. V. Ozmidov, "On the turbulent exchange in a stably stratified ocean," *Izv., Acad. Sci., USSR, Atmos. Oceanic Phys.* **1**, 853–860 (1965).
- <sup>4</sup>T. M. Dillon, "Vertical overturns: A comparison of Thorpe and Ozmidov length scales," *J. Geophys. Res.* **87**, 9601–9613, doi:10.1029/JC087iC12p09601 (1982).
- <sup>5</sup>S. A. Thorpe, *The Turbulent Ocean* (Cambridge University Press, 2005).
- <sup>6</sup>T. H. Ellison, "Turbulent transport of heat and momentum from an infinite rough plane," *J. Fluid Mech.* **2**, 456–466 (1957).
- <sup>7</sup>E. C. Itsweire, "Measurements of vertical overturns in a stably stratified turbulent flow," *Phys. Fluids* **27**(4), 764–766 (1984).
- <sup>8</sup>E. C. Itsweire, J. R. Koseff, D. A. Briggs, and J. H. Ferziger, "Turbulence in stratified shear flows: Implications for interpreting shear-induced mixing in the ocean," *J. Phys. Oceanogr.* **23**, 1508–1522 (1993).
- <sup>9</sup>S. B. Pope, *Turbulent Flows* (Cambridge University Press, 2000).
- <sup>10</sup>S. Corrsin, "On local isotropy in turbulent shear flow," NACA RM **58B11**, 1–15 (1958).
- <sup>11</sup>A. N. Kolmogorov, "A refinement of previous hypotheses concerning the local structure of turbulence in a viscous incompressible fluid at high Reynolds number," *J. Fluid Mech.* **13**(1), 82–85 (1962).
- <sup>12</sup>C. H. Gibson, "Fossil temperature, salinity, and vorticity turbulence in the ocean," in *Marine Turbulence*, edited by J. C. Nihoul (Elsevier Publishing Co., Amsterdam, 1980), Vol. 28, pp. 221–257.
- <sup>13</sup>L. H. Shih, J. R. Koseff, G. N. Ivey, and J. H. Ferziger, "Parameterization of turbulent fluxes and scales using homogeneous sheared stably stratified turbulence simulations," *J. Fluid Mech.* **525**, 193–214 (2005).
- <sup>14</sup>D. C. Stillinger, K. N. Helland, and C. W. V. Atta, "Experiments on the transition of homogeneous turbulence to internal waves in a stratified fluid," *J. Fluid Mech.* **131**, 91–122 (1983).
- <sup>15</sup>G. N. Ivey, K. B. Winters, and J. R. Koseff, "Density stratification, turbulence, but how much mixing?" *Annu. Rev. Fluid Mech.* **40**, 169–184 (2008).
- <sup>16</sup>J. J. Riley, R. W. Metcalfe, and M. A. Weissman, "Direct numerical simulations of homogeneous turbulence in density stratified fluids," *AIP Conf. Proc.* **76**, 79–112 (1981).
- <sup>17</sup>S. K. Venayagamoorthy and D. D. Stretch, "Lagrangian mixing in decaying stably stratified turbulence," *J. Fluid Mech.* **564**, 197–226 (2006).
- <sup>18</sup>W. Smyth and J. Moum, "Length scales of turbulence in stably stratified mixing layers," *Phys. Fluids* **12**(6), 1327–1342 (2000).
- <sup>19</sup>K. B. Winters, P. N. Lombard, J. J. Riley, and E. A. D'Asaro, "Available potential energy and mixing in density-stratified flows," *J. Fluid Mech.* **289**, 115–128 (1995).
- <sup>20</sup>W. Smyth, J. Moum, and D. Caldwell, "The efficiency of mixing in turbulent patches: Inferences from direct simulations and microstructure observations," *J. Phys. Oceanogr.* **31**(8), 1969–1992 (2001).
- <sup>21</sup>B. Ferron, H. Mercier, K. Speer, A. Gargett, and K. Polzin, "Mixing in the romanche fracture zone," *J. Phys. Oceanogr.* **28**, 1929–1945 (1998).
- <sup>22</sup>D. Luketina and J. Imberger, "Turbulence and entrainment in a buoyant surface plume," *J. Geophys. Res.* **94**(C9), 12619–12636, doi:10.1029/JC094iC09p12619 (1989).
- <sup>23</sup>G. N. Ivey and J. Imberger, "On the nature of turbulence in a stratified fluid. Part I: The energetics of mixing," *J. Phys. Oceanogr.* **21**, 650–659 (1991).
- <sup>24</sup>S. K. Venayagamoorthy and D. D. Stretch, "On the turbulent Prandtl number in homogeneous stably stratified turbulence," *J. Fluid Mech.* **644**, 359–369 (2010).
- <sup>25</sup>E. C. Itsweire, K. N. Helland, and C. W. V. Atta, "The evolution of grid-generated turbulence in a stably stratified fluid," *J. Fluid Mech.* **162**, 299–338 (1986).
- <sup>26</sup>J. N. Moum, "Energy-containing scales of turbulence in the ocean thermocline," *J. Geophys. Res.* **101**(C6), 14095–14109, doi:10.1029/96JC00507 (1996).